

See discussions, stats, and author profiles for this publication at: <https://www.researchgate.net/publication/45797060>

A Robust Highly Interpenetrated Metal–Organic Framework Constructed from Pentanuclear Clusters for Selective Sorption of Gas Molecules

ARTICLE *in* INORGANIC CHEMISTRY · SEPTEMBER 2010

Impact Factor: 4.76 · DOI: 10.1021/ic1010083 · Source: PubMed

CITATIONS

50

READS

40

7 AUTHORS, INCLUDING:



Yu-Sheng Chen

University of Chicago

120 PUBLICATIONS 1,449 CITATIONS

SEE PROFILE



Banglin Chen

University of Texas at San Antonio

160 PUBLICATIONS 17,943 CITATIONS

SEE PROFILE

A Robust Highly Interpenetrated Metal–Organic Framework Constructed from Pentanuclear Clusters for Selective Sorption of Gas Molecules

Zhangjing Zhang,[†] Shengchang Xiang,^{*,†} Yu-Sheng Chen,[‡] Shengqian Ma,^{‡,#} Yongwoo Lee,[§] Thomas Phely-Bobin,[§] and Banglin Chen^{*,†}

[†]Department of Chemistry, University of Texas at San Antonio, One UTSA Circle, San Antonio, Texas 78249-0698,

[‡]ChemMatCARS, Center for Advanced Radiation Sources, The University of Chicago, 9700 S. Cass Avenue, Argonne, Illinois 60439, and [§]QinetiQ North America, Technology Solutions Group, 360 Second Avenue, Waltham,

Massachusetts 02451. [#]Current address: Department of Chemistry, University of South Florida, Tampa, Florida 33620.

Received May 19, 2010

A three-dimensional microporous metal–organic framework, $\text{Zn}_5(\text{BTA})_6(\text{TDA})_2 \cdot 15\text{DMF} \cdot 8\text{H}_2\text{O}$ (**1**; HBTa = 1,2,3-benzenetriaazole; H_2TDA = thiophene-2,5-dicarboxylic acid), comprising pentanuclear $[\text{Zn}_5]$ cluster units, was obtained through an one-pot solvothermal reaction of $\text{Zn}(\text{NO}_3)_2$, 1,2,3-benzenetriaazole, and thiophene-2,5-dicarboxylate. The activated **1** displays type-I N_2 gas sorption behavior with a Langmuir surface area of $607 \text{ m}^2 \text{ g}^{-1}$ and exhibits interesting selective gas adsorption for $\text{C}_2\text{H}_2/\text{CH}_4$ and CO_2/CH_4 .

Introduction

Porous metal–organic frameworks (MOFs) have been emerging as very promising materials for gas storage, separation,

heterogeneous catalysis, sensing, and drug delivery over the past two decades.^{1–41} The diverse metal ions and/or metal-containing clusters as the nodes and a variety of organic linkers as the bridges to construct the porous coordination polymers (PCPs) by the coordination bonds have led to a series of porous MOFs from ultramicroporous to mesoporous domains. Although extensive research has been carried out to assemble the coordination polymers, those exhibiting permanent porosity and thus being classified as porous MOFs are still of few percentage. This is mainly

*To whom correspondence should be addressed. E-mail: shengchang.xiang@utsa.edu (S.X.), banglin.chen@utsa.edu (B.C.).

(1) Eddaoudi, M.; Moler, D. B.; Li, H.; Chen, B.; Reineke, T. M.; O'Keeffe, M.; Yaghi, O. M. *Acc. Chem. Res.* **2001**, *34*, 319. Kitagawa, S.; Kitaura, R.; Noro, S. *Angew. Chem., Int. Ed.* **2004**, *43*, 2334. Bradshaw, D.; Claridge, J. B.; Cussen, E. J.; Prior, T. J.; Rosseinsky, M. J. *Acc. Chem. Res.* **2005**, *38*, 273. Ma, L.; Abney, C.; Lin, W. *Chem. Soc. Rev.* **2009**, *38*, 1248. Férey, G. *Chem. Soc. Rev.* **2008**, *37*, 191. Suh, M. P.; Cheon, Y. E.; Lee, E. Y. *Coord. Chem. Rev.* **2008**, *252*, 1007. Czaja, A. U.; Trukhan, N.; Müller, U. *Chem. Soc. Rev.* **2009**, *38*, 1284. Chen, B.; Xiang, S. C.; Qian, G. D. *Acc. Chem. Res.* **2010**, DOI: 10.1021/ar100023y.

(2) Zhang, J. P.; Chen, X. M. *J. Am. Chem. Soc.* **2008**, *130*, 6010. Zhu, A. X.; Lin, J. B.; Zhang, J. P.; Chen, X. M. *Inorg. Chem.* **2009**, *48*, 3882.

(3) Wu, T.; Bu, X.; Liu, R.; Lin, Z.; Zhang, J.; Feng, P. *Chem.–Eur. J.* **2008**, *14*, 7771. Zhang, J.; Wu, T.; Zhou, C.; Chen, S.; Feng, P.; Bu, X. *Angew. Chem., Int. Ed.* **2009**, *48*, 2542.

(4) Choi, E. Y.; Barron, P. M.; Novotny, R. W.; Son, H. T.; Hu, C.; Choe, W. *Inorg. Chem.* **2009**, *48*, 426.

(5) Lin, X.; Telepeni, I.; Blake, A. J.; Dailly, A.; Brown, C. M.; Simmons, J. M.; Zoppi, M.; Walker, G. S.; Thomas, K. M.; Mays, T. J.; Hubberstey, P.; Champness, N. R.; Schröder, M. *J. Am. Chem. Soc.* **2009**, *131*, 2159.

(6) Chandler, B. D.; Cramb, D. T.; Shimizu, G. K. H. *J. Am. Chem. Soc.* **2006**, *128*, 10403.

(7) Park, Y. K.; Choi, S. B.; Kim, H.; Kim, K.; Won, B.-H.; Choi, K.; Choi, J.-S.; Ahn, W.-S.; Won, N.; Kim, S.; Jung, D. H.; Choi, S.-H.; Kim, G.-H.; Cha, S.-S.; Jhon, Y. H.; Yang, J. K.; Kim, J. *Angew. Chem., Int. Ed.* **2007**, *46*, 8230.

(8) Farha, O. K.; Spokoyny, A. M.; Mulfort, K. L.; Hawthorne, M. F.; Mirkin, C. A.; Hupp, J. T. *J. Am. Chem. Soc.* **2007**, *129*, 12680.

(9) Huang, G.; Yang, C.; Xu, Z.; Wu, H.; Li, J.; Zeller, M.; Hunter, A. D.; Chui, S. S. Y.; Che, C. M. *Chem. Mater.* **2009**, *21*, 541.

(10) Fang, Q.-R.; Zhu, G.-S.; Jin, Z.; Xue, M.; Wei, X.; Wang, D.-J.; Qiu, S.-L. *Angew. Chem.* **2006**, *118*, 6272. Fang, Q. R.; Zhu, G. S.; Xue, M.; Zhang, Q. L.; Sun, J. Y.; Guo, X. D.; Qiu, S. L.; Xu, S. T.; Wang, P.; Wang, D. J.; Wei, Y. *Chem.–Eur. J.* **2006**, *12*, 3754.

(11) Bai, Y.-L.; Tao, J.; Huang, R.-B.; Zheng, L.-S. *Angew. Chem., Int. Ed.* **2008**, *47*, 5344. Wang, X.-L.; Qin, C.; Wu, S.-X.; Shao, K.-Z.; Lan, Y.-Q.; Wang, S.; Zhu, D.-X.; Su, Z.-M.; Wang, E.-B. *Angew. Chem., Int. Ed.* **2009**, *48*, 5291.

(12) Eddaoudi, M.; Li, H.; Yaghi, O. M. *J. Am. Chem. Soc.* **2000**, *122*, 1391.

(13) Ma, L.; Lin, W. *Angew. Chem., Int. Ed.* **2009**, *48*, 3637. Kesanli, B.; Cui, Y.; Smith, M. R.; Bittner, E. W.; Bockrath, B. C.; Lin, W. *Angew. Chem., Int. Ed.* **2005**, *44*, 72.

(14) Ma, S.; Sun, D.; Ambrogio, M.; Fillinger, J. A.; Parkin, S.; Zhou, H.-C. *J. Am. Chem. Soc.* **2007**, *129*, 1858–1859. Ma, S.; Eckert, J.; Forster, P. M.; Yoon, J. W.; Hwang, Y. K.; Chang, J.-S.; Collier, C. D.; Parise, J. B.; Zhou, H.-C. *J. Am. Chem. Soc.* **2008**, *130*, 15896–15902.

(15) Roswell, J.; Yaghi, O. M. *J. Am. Chem. Soc.* **2006**, *128*, 1304.

(16) Xiang, S. C.; Zhou, W.; Gallegos, J. M.; Liu, Y.; Chen, B. *J. Am. Chem. Soc.* **2009**, *131*, 12415.

(17) Xiang, S. C.; Zhou, W.; Zhang, Z.-J.; Green, M. A.; Liu, Y.; Chen, B. *Angew. Chem., Int. Ed.* **2010**, *49*, 4615–4618.

(18) Bastin, L.; Barcia, P. S.; Hurtado, E. J.; Silva, A. C.; Rodrigues, A. E.; Chen, B. *J. Phys. Chem. C* **2008**, *112*, 1575.

(19) Wang, B.; Côté, A. P.; Furukawa, H.; O'Keeffe, M.; Yaghi, O. M. *Nature* **2008**, *453*, 207.

(20) Choi, H.-S.; Suh, M. P. *Angew. Chem., Int. Ed.* **2009**, *48*, 6865.

(21) An, J.; Geib, S. J.; Rosi, N. L. *J. Am. Chem. Soc.* **2010**, *132*, 38.

(22) Wu, H.; Zhou, W.; Yildirim, T. *J. Am. Chem. Soc.* **2009**, *131*, 4995.

(23) Nouar, F.; Eubank, J. F.; Bousquet, T.; Wojtas, L.; Zaworotko, M. J.; Eddaoudi, M. *J. Am. Chem. Soc.* **2008**, *130*, 1833.

because of the labile coordination geometries of the metal ions and/or metal-containing clusters and the flexibility of the bridging organic linkers which cannot sustain the frameworks under vacuum and/or thermal activation. One efficient strategy to stabilize the PCPs and thus to construct porous MOFs is to make use of rigid clusters,^{10,11} as exemplified in those MOFs with the binuclear paddle-wheel $M_2(\text{COO})_6$ ($M = \text{Cu}^{2+}$, Co^{2+} , Ni^{2+} , and Zn^{2+}) and tetranuclear $\text{Zn}_4\text{O}(\text{COO})_6$ as the secondary building units.¹² Another strategy to stabilize the frameworks is to make use of the framework interpenetration and/or interwoven to enforce the framework interactions.¹³ In fact, quite a few examples of porous MOFs have been realized by this approach in which the interpenetrated/interwoven frameworks show a higher permanent porosity than their noninterpenetrated framework analogues.¹⁴

Herein we report a rare example of porous MOF $\text{Zn}_5(\text{BTA})_6(\text{TDA})_2 \cdot 15\text{DMF} \cdot 8\text{H}_2\text{O}$ (**1**; $\text{HBTA} = 1,2,3\text{-benzenetriazole}$; $\text{H}_2\text{TDA} = \text{thiophene-2,5-dicarboxylic acid}$) in which both the rigid pentanuclear $\text{Zn}_5(\text{BTA})_6$ cluster and the four-fold framework interpenetration have been cooperatively utilized to stabilize the framework, exhibiting highly selective sorption behavior toward $\text{C}_2\text{H}_2/\text{CH}_4$ and CO_2/CH_4 .

Experimental Section

Materials and Methods. All reagents and solvents employed were commercially available and used as supplied without further purification. Thermogravimetric analysis (TGA) data were obtained on a TGA G500 V5.3 Build 171 instrument with a heating rate of $5^\circ\text{C}/\text{min}$ under a N_2 atmosphere. Powder X-ray diffraction (XRD) patterns were obtained with a Scintag X1 powder diffractometer system using $\text{K}\alpha$ radiation with a variable divergent slit and a solid-state detector. The routine power was 1400 W (40 kV, 35 mA). Low-background quartz XRD slides (Gem Depot, Inc., Pittsburgh, PA) were used. For analyses, powder samples were dispersed on glass slides.

Synthesis of MOF 1. A mixture of $\text{Zn}(\text{NO}_3)_2 \cdot 6\text{H}_2\text{O}$ (1.487 g, 5 mmol), HBTA (0.715 g, 6 mmol), and H_2TDA (0.344 g, 2 mmol) were dissolved in the mixed DMF–ethanol–water (70/70/70 mL) solution and heated in a vial (400 mL) at 100°C for 24 h. The colorless octahedron-shaped crystals formed were collected, washed with DMF, and dried in air (1.883 g; yield: 72%). Elem. anal. calcd for $\text{Zn}_5(\text{BTA})_6(\text{TDA})_2 \cdot 15\text{DMF} \cdot 8\text{H}_2\text{O}$ ($\text{C}_{93}\text{H}_{149}\text{N}_{33}\text{O}_{31}\text{S}_2\text{Zn}_5$): C, 42.69; H, 5.74; N, 17.67. Found: C, 42.84; H, 5.81; N, 17.65. Sample of MOF **1** was soaked in methanol, filtered, and activated under high vacuum at 150°C overnight to get MOF **1a**.

Single-Crystal X-ray Crystallography. Single crystal X-ray data of MOF **1** were collected using the microcrystal diffraction beamline 15ID-B at the Advanced Photon Source, Argonne National Laboratory (ANL). Data were collected on a Bruker D8 diffractometer equipped with an APEX II detector. Data integration and reduction were using the APEX suite software. The structure was solved by direct methods and subsequent difference Fourier syntheses and refined using the SHELXTL software package. The H atoms on the ligand were placed in idealized positions and refined using a riding model. The H atoms on the coordinated solvent O atoms could not be located. The unit cell includes a large region of disordered solvent molecules, which could not be modeled as discrete atomic sites. We employed PLATON/SQUEEZE to calculate the diffraction contribution of the solvent molecules and thereby producing a set of solvent-free diffraction intensities.⁴²

Gas Sorption Measurements. A Micromeritics ASAP 2020 surface area analyzer was used to measure gas adsorption. In order to remove guest solvent molecules in the framework, the fresh sample soaked in methanol was filtered and vacuumed at 150°C overnight. A sample of 150.0 mg was used for the sorption measurement and was maintained at 77 K with liquid nitrogen and 273 K with ice–water bath (slush), respectively. As the center-controlled air condition was set up at 22.0°C , a water bath of 22.0°C was used for adsorption isotherms at 295.0 K.

Derivation of the Isothermic Heats of Adsorption. A virial-type expression of the following form was used to fit the combined isotherm data for a given material at 295.0 and 273.2 K:^{15,16}

$$\ln P = \ln N + 1/T \sum_{i=0}^m a_i N^i + \sum_{i=0}^n b_i N^i \quad (1)$$

(42) Roquerol, F.; Rouquerol, J.; Sing, K. *Adsorption by Powders and Solids: Principles, Methodology, and Applications*; Academic Press: London, 1999.

- (24) Chen, B.; Liang, C.; Yang, J.; Contreras, D. S.; Clancy, Y. L.; Lobkovsky, E. B.; Yaghi, O. M.; Dai, S. *Angew. Chem., Int. Ed.* **2006**, *45*, 1390. Chen, B.; Ma, S.; Zapata, F.; Fronczek, F. R.; Lobkovsky, E. B.; Zhou, H. C. *Inorg. Chem.* **2007**, *46*, 1233. Chen, B.; Ma, S.; Hurtado, E. J.; Lobkovsky, E. B.; Zhou, H. C. *Inorg. Chem.* **2007**, *46*, 8490. Chen, B.; Ma, S.; Hurtado, E. J.; Lobkovsky, E. B.; Liang, C.; Zhu, H.; Dai, S. *Inorg. Chem.* **2007**, *46*, 8705. Barcia, P. S.; Zapata, F.; Silva, J. A. C.; Rodrigues, A. E.; Chen, B. *J. Phys. Chem. B* **2007**, *111*, 6101. Xue, M.; Ma, S. Q.; Jin, Z.; Schaffino, R. M.; Zhu, G. S.; Lobkovsky, E. B.; Qiu, S. L.; Chen, B. *Inorg. Chem.* **2008**, *47*, 6825. Chen, B.; Zhao, X.; Putkham, A.; Hong, K.; Lobkovsky, E. B.; Hurtado, E. J.; Fletcher, A. J.; Thomas, K. M. *J. Am. Chem. Soc.* **2008**, *130*, 6411. Chen, Z.; Xiang, S.; Zhao, D.; Chen, B. *Cryst. Growth Des.* **2009**, *9*, 5293. Xue, M.; Zhang, Z.-J.; Xiang, S.-C.; Jin, Z.; Liang, C.; Zhu, G.-S.; Qiu, S.-L.; Chen, B. *J. Mater. Chem.* **2010**, *20*, 3984.
- (25) Pan, L.; Parker, B.; Huang, X.; Olson, D. H.; Lee, J.; Li, J. *J. Am. Chem. Soc.* **2006**, *128*, 4180. Pan, L.; Olson, D. H.; Ciemnomolowski, L. R.; Heddy, R.; Li, J. *Angew. Chem., Int. Ed.* **2006**, *45*, 616. Li, K.; Olson, D. H.; Seidel, J.; Emge, T. J.; Gong, H.; Zeng, H.; Li, J. *J. Am. Chem. Soc.* **2009**, *131*, 10368.
- (26) Pan, L.; Adams, K. M.; Hernandez, H. E.; Wang, X.; Zheng, C.; Hattori, Y.; Kaneko, K. *J. Am. Chem. Soc.* **2003**, *125*, 3062.
- (27) Dybtsev, D. N.; Chun, H.; Yoon, S. H.; Kim, D.; Kim, K. *J. Am. Chem. Soc.* **2004**, *126*, 32. Kim, H.; Samsonenko, D. G.; Yoon, M.; Yoon, J. W.; Hwang, Y. K.; Chang, J. S.; Kim, K. *Chem. Commun.* **2008**, 4697.
- (28) Kitaura, R.; Seki, K.; Akiyama, G.; Kitagawa, S. *Angew. Chem., Int. Ed.* **2003**, *42*, 428. Matsuda, R.; Kitaura, R.; Kitagawa, S.; Kubota, Y.; Belosludov, R. V.; Kobayashi, T. C.; Sakamoto, H.; Chiba, T.; Takata, M.; Kawazoe, Y.; Mita, Y. *Nature* **2005**, *436*, 238.
- (29) Dinca, M.; Long, J. R. *J. Am. Chem. Soc.* **2005**, *127*, 9376.
- (30) Bourrelly, S.; Llewellyn, P. L.; Serre, C.; Millange, F.; Loiseau, T.; Férey, G. *J. Am. Chem. Soc.* **2005**, *127*, 13519.
- (31) Navarro, J. A. R.; Barea, E.; Salas, J. M.; Masciocchi, N.; Galli, S.; Sironi, A.; Ania, C. O.; Parra, J. B. *Inorg. Chem.* **2006**, *45*, 2397.
- (32) Bae, Y. S.; Farha, O. K.; Spokoyny, A. M.; Mirkin, C. A.; Hupp, J. T.; Snurr, R. Q. *Chem. Commun.* **2008**, 4135. Bae, Y. S.; Farha, O. K.; Hupp, J. T.; Snurr, R. Q. *J. Mater. Chem.* **2009**, *19*, 2131.
- (33) Ma, S.; Sun, D.; Wang, X. S.; Zhou, H. C. *Angew. Chem., Int. Ed.* **2007**, *46*, 2458. Ma, S.; Wang, X. S.; Collier, C. D.; Manis, E. S.; Zhou, H. C. *Inorg. Chem.* **2007**, *46*, 8499. Ma, S.; Sun, D.; Yuan, D.; Wang, X. S.; Zhou, H. C. *J. Am. Chem. Soc.* **2009**, *131*, 6445. Ma, S.; Yuan, D.; Wang, X. S.; Zhou, H. C. *Inorg. Chem.* **2009**, *48*, 2072. Ma, S.; Wang, X. S.; Yuan, D.; Zhou, H. C. *Angew. Chem., Int. Ed.* **2008**, *47*, 4130.
- (34) Humphrey, S. M.; Chang, J. S.; Jhung, S. H.; Yoon, J. W.; Wood, P. T. *Angew. Chem., Int. Ed.* **2007**, *46*, 272.
- (35) Li, J. R.; Tao, Y.; Yu, Q.; Bu, X. H.; Sakamoto, H.; Kitagawa, S. *Chem.–Eur. J.* **2008**, *14*, 2771.
- (36) Banerjee, R.; Furukawa, H.; Britt, D.; Knobler, C.; O’Keeffe, M.; Yaghi, O. M. *J. Am. Chem. Soc.* **2009**, *131*, 3875.
- (37) Zou, Y.; Hong, S.; Park, M.; Chun, H.; Lah, M. S. *Chem. Commun.* **2007**, 5182. Couck, S.; Denayer, J. F. M.; Baron, G. V.; Rémy, T.; Gascon, J.; Kapteijn, F. *J. Am. Chem. Soc.* **2009**, *131*, 6326.
- (38) Myers, A. L.; Prausnitz, J. M. *AIChE J.* **1965**, *11*, 121. Mu, B.; Li, F.; Walton, K. S. *Chem. Commun.* **2009**, 2493. Lee, J. Y.; Roberts, J. M.; Farha, O. K.; Sarjeant, A. A.; Scheidt, K. A.; Hupp, J. T. *Inorg. Chem.* **2009**, *48*, 9971. Babarao, R.; Hu, Z. Q.; Jiang, J. W.; Chempath, S.; Sandler, S. I. *Langmuir* **2007**, *23*, 659. Yang, Q. Y.; Zhong, C. L. *J. Phys. Chem. B* **2006**, *110*, 17776.
- (39) Tranchemontagne, D. J.; Mendoza-Cortes, J. L.; O’Keeffe, M.; Yaghi, O. M. *Chem. Soc. Rev.* **2009**, *38*, 1257.
- (40) Li, J. R.; Kuppler, R. J.; Zhou, H. C. *Chem. Soc. Rev.* **2009**, *38*, 1477.
- (41) Spek, A. L. *J. Appl. Crystallogr.* **2003**, *36*, 7.

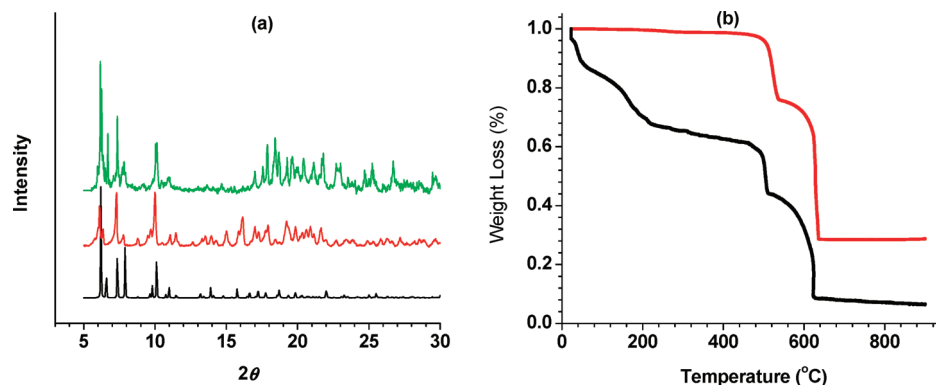


Figure 1. (a) Powder XRD for MOF **1**: simulated pattern (black), as-synthesized (green), and activated (**1a**) samples at 150 °C (red). (b) TGA curve for MOF **1**: as-synthesized (black) and activated **1a** (red) samples.

Here, P is the pressure expressed in Torr, N is the amount adsorbed in mmol/g, T is the temperature in K, a_i and b_i are virial coefficients, and m and n represent the number of coefficients required to adequately describe the isotherms. The equation was fit using the statistical software package SPSS 16.0. The coefficients m and n were gradually increased until the contribution of extra added a and b coefficients was deemed to be statistically insignificant toward the overall fit, as determined using the average value of the squared deviations from the experimental values was minimized. In all cases, $m \leq 6$ and $n \leq 3$. The values of the virial coefficients a_0 through a_m were then used to calculate the isosteric heat of adsorption using the following expression:

$$Q_{st} = -R \sum_{i=0}^m a_i N^i \quad (2)$$

Here, Q_{st} is the coverage-dependent isosteric heat of adsorption, and R is the universal gas constant of $8.3147 \text{ J K}^{-1} \text{ mol}^{-1}$.

Results and Discussion

The MOF **1** was synthesized by the solvothermal reaction of zinc nitrate, HBTa, and H_2TDA in a mixture solvent of DMF/ $\text{C}_2\text{H}_5\text{OH}/\text{H}_2\text{O}$ at 100 °C for 24 h as colorless octahedral crystals. It was formulated as $\text{Zn}_5(\text{BTA})_6(\text{TDA})_2 \cdot 15\text{DMF} \cdot 8\text{H}_2\text{O}$ by elemental microanalysis and single-crystal X-ray diffraction studies, and the phase purity of the bulk material was independently confirmed by powder X-ray diffraction (PXRD) (Figure 1a) and thermogravimetric analysis (TGA) (Figure 1b).

A single-crystal X-ray crystallographic study, conducted using synchrotron microcrystal diffraction at the Advanced Photon Source, ANL, revealed that **1** crystallizes in a tetragonal space group $I4_1/a$. Also **1** is a three-dimensional (3D) open-framework comprising $\{\text{Zn}_5(\text{BTA})_6(\text{O}_{\text{solvent}})\}$ clusters as tetrahedral nodes, which were linked to four crystallographically independent clusters by the extended TDA ligands via their carboxylate groups to give a *diamond* network (Figure 2). Within the $\{\text{Zn}_5(\text{BTA})_6(\text{O}_{\text{solvent}})_4\}$ cluster, a Zn3 ion located at the center is surrounded by six N atoms from six BTAs, while the coordination environments of the other four at each vertex of the tetrahedron were completed by three N atoms from 3 BTAs and two O atoms from TDA linkers. One of the four vertical Zn ions (Zn4) is further bounded to one O atom of the solvent molecule, indicating the potential to have the open metal sites for their recognition of the gas molecules once the MOF **1** was thermally activated. The adamantanoid cages in a single dia net have a dimension of ca. 26 Å in diameter. The spacious nature of the single

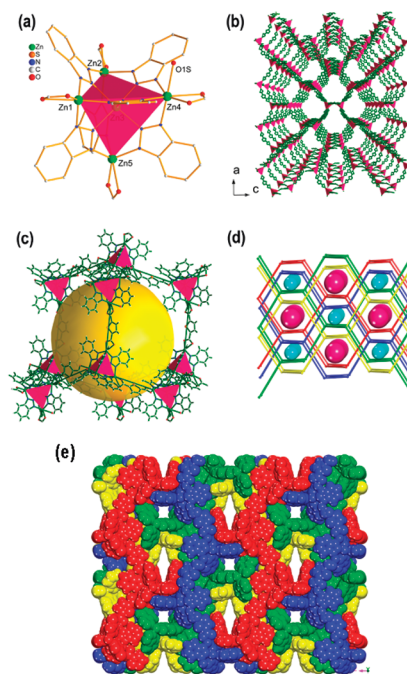


Figure 2. Each $\{\text{Zn}_5(\text{BTA})_6(\text{O}_{\text{solvent}})\}$ cluster (a) was linked by four TDA molecules to form a single dia net (b) viewed down the b axis, comprising large adamantanoid cages (c, yellow); (d) Four-fold interpenetration diamond networks give two kinds of channels along both a and b axes: a long and narrow one, (pink) sites between the yellow and red networks and another quasisquare one (cyan), between the blue and green networks; and (e) Four-fold interpenetrated framework exhibiting the channels along the a axis.

network allows three other identical dia networks to penetrate it in a normal mode, thus resulting in a four-fold interpenetrating dia array (Figure 2d). Despite the interpenetration, the framework of **1** remains open and contains 1D channels of ca. $4.1 \times 10.0 \text{ Å}^2$ (pink) and $3.4 \times 4.1 \text{ Å}^2$ (cyan) along the $[1\ 0\ 0]$ and $[0\ 1\ 0]$ directions that are occupied by disordered solvent molecules. PLATON⁴² analysis showed that the effective free volume of **1** is 37% of the crystal volume.

TGA of MOF **1** showed that approximately 40% weight loss occurred from 23 to 450 °C, which is attributed primarily to the release of solvent molecules and coordinated solvent molecules (Figure 1b). PXRD studies indicate that the activated **1** (MOF **1a**) at 150 °C under high vacuum overnight keeps the high-crystalline feature whose pattern matches with that of the as-synthesized **1**, indicating that the framework of

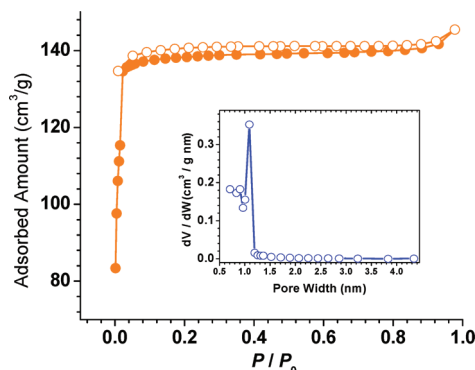


Figure 3. Isothermal adsorption curve of N_2 gas for **1a**. Inset: Horvath–Kawazoe pore size distribution plot.

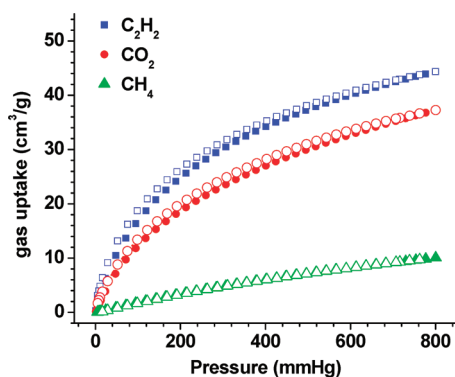


Figure 4. Adsorption (solid) and desorption (open) isotherms of activated **1** at 295 K (acetylene (blue); carbon dioxide (red); and methane (green)).

1 is robust. N_2 sorption isotherm at 77 K shows that the **1a** displays typical type-I sorption behavior with the Brunauer–Emmett–Teller (BET) surface area of $414 \text{ m}^2 \text{ g}^{-1}$ (Langmuir surface area, $607 \text{ m}^2 \text{ g}^{-1}$) and pore volume of $0.24 \text{ cm}^3 \text{ g}^{-1}$ (estimated by using Dubinin–Radushkevich equation), respectively (Figure 3).⁴³ A fit of the adsorption data to the Horvath–Kawazoe model shows the maximum pore size in the range of 1.0–1.1 nm, in agreement with the structural analysis above.

The establishment of permanent porosity of **1a** enables us to examine its potential application on the selective gas separation. As shown in Figure 4, **1a** can take differential amounts of C_2H_2 ($44 \text{ cm}^3/\text{g}$), CO_2 ($37 \text{ cm}^3/\text{g}$), and CH_4 ($10 \text{ cm}^3/\text{g}$) at 1 atm and 295 K, highlighting **1a** as the promising material for the selective separation of C_2H_2/CH_4 and CO_2/CH_4 at room temperature. Such selective sorption of **1a** with respect to these three gas molecules are mainly attributed to their different interactions with the framework surfaces.

The coverage-dependent adsorption enthalpies of **1a** to these three gases, calculated based on virial method, a well established and reliable methodology from fits of their adsorption isotherms at 273 and 295 K. The enthalpies at zero coverage are 37.3, 37.8, and 26.1 kJ/mol for C_2H_2 , CO_2 , and CH_4 , respectively (Figure 5). These values of adsorption enthalpies are systematically high. In fact, the acetylene adsorption enthalpy **1a** is much higher than that of 24.0 kJ/mol

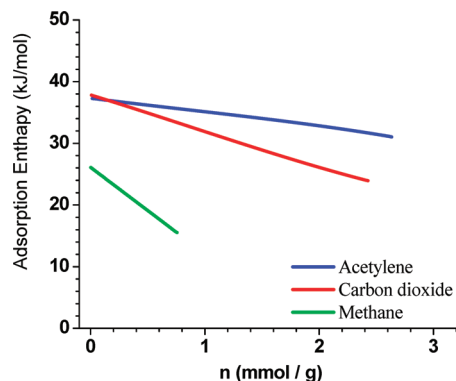


Figure 5. The heat of adsorption of the activated **1** for acetylene (blue), carbon dioxide (red), and methane (green).

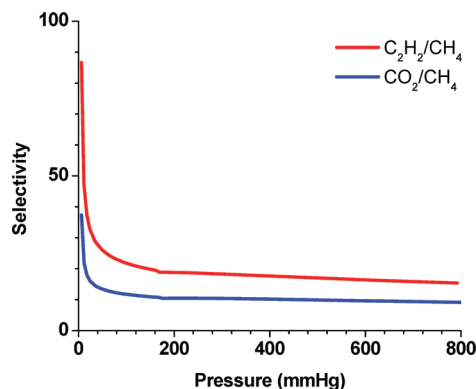


Figure 6. Selectivity of C_2H_2/CH_4 (red) and CO_2/CH_4 (blue) in **1a** for equimolar mixtures at 295 K.

of Zn-MOF-74 with well orientated open Zn^{2+} sites.¹⁷ Such systematically larger enthalpies for gas adsorption might be attributed to both the possible open $Zn4$ sites and the optimized the pore surface/curvature for their enhanced interactions with the gas molecules.

The separation capabilities of **1a** for the selective CO_2/CH_4 and C_2H_2/CH_4 separation have been further examined by the ideal adsorbed solution theory (IAST). The calculated IAST selectivities³⁹ are shown in Figure 6. The Langmuir–Freundlich model was applied to fit the experimental isotherms with excellent results ($R > 0.999$), and IAST calculations were performed under equimolar mixture conditions. It was found that **1a** displays very high selectivities for CO_2 at low pressure. At about 6 mmHg, the CO_2/CH_4 and C_2H_2/CH_4 separation selectivity is 37 and 87, respectively. The selectivity decreases with increasing bulk pressure as zinc sites become inaccessible. The calculated selectivity for equimolar CO_2/CH_4 and C_2H_2/CH_4 is about 9.2 and 15.5, respectively, at 1 atm and 295 K, while the Henry's selectivities obtained from the virial method toward CO_2/CH_4 and C_2H_2/CH_4 are respectively 12.0 and 22.3 at 295 K (Supporting Information, Table S2). These values are moderately high compared with those of well examined microporous MOFs.³⁹ The possible open $Zn4$ sites within **1a** may enforce their stronger interactions with C_2H_2 and CO_2 .

To make use of the pentanuclear cluster and four-fold framework interpenetration, we realize a robust microporous metal–organic framework (MOF) for highly selective separation of C_2H_2/CH_4 and CO_2/CH_4 . The rich cluster chemistry to provide the stable nodes for the construction of porous

(43) Xie, L.-H.; Lin, J.-B.; Liu, X.-M.; Wang, Y.; Zhang, W.-X.; Zhang, J.-P.; Chen, X.-M. *Inorg. Chem.* **2010**, *49*, 1158.

MOFs⁴⁰ and the power of the framework interpenetration/interwoven to stabilize and then tune the porosity of the synthesized MOFs will enrich a variety of new porous MOFs for gas separation, one of the most promising applications of the emerging porous MOFs for the industrial and environmental usage in the near future.⁴¹

Acknowledgment. This work was supported by an Award CHE 0718281 from the NSF, AX-1730 from Welch Foundation (BC). ChemMatCARS Sector 15 is principally supported by the National Science Foundation/Department of Energy under Grant No. NSF/CHE-0822838. Use of the Advanced Photon Source was sup-

ported by the U.S. Department of Energy, Office of Science, Office of Basic Energy Sciences, under Contract No. DE-AC02-06CH11357. The views, opinions, and/or findings contained in this article/presentation are those of the author/presenter and should not be interpreted as representing the official views or policies, either expressed or implied, of the Defense Advanced Research Projects Agency or the Department of Defense.

Supporting Information Available: The adsorption and desorption isotherms of MOF **1a** at 273 K, the virial graphs and the virial coefficients. This material is available free of charge via the Internet at <http://pubs.acs.org>.